Coupling a magnetic bottle multi-electron spectrometer with a liquid micro-jet device: a comprehensive study of solvated sodium benzoate at the O 1 s threshold

Marine Fournier, Lucie Huart, Rémi Dupuy, Régis Vacheresse, Maximilian Reinhardt, Denis Cubaynes, Denis Céolin, Marie-Anne Hervé Du Penhoat, Jean-Philippe Renault, Jean-Michel Guigner, et al.

HAL Id: hal-03924957

https://hal.sorbonne-universite.fr/hal-03924957

Submitted on 8 Feb 2024

Coupling a magnetic bottle multi-electron spectrometer with a liquid micro-jet device: a comprehensive study of solvated sodium benzoate at the O 1*s* threshold

Marine Fournier[1,2], *Lucie* Huart[2,3,4], *Rémi* Dupuy[1,5], *Régis* Vacheresse[1], *Maximilian* Reinhardt[6], *Denis* Cubaynes[7], *Denis* Céolin[2], *Marie-Anne* Hervé du Penhoat[4], *Jean-Philippe* Renault[3], *Jean-Michel* Guigner[4], *Ajit* Kumar[2], *Bastien* Lutet-Toti[1], *John* Bozek[2], *Iyas* Ismail[1], *Loïc* Journel[1], *Pascal* Lablanquie[1], *Francis* Penent[1], *Christophe* Nicolas[2] and *Jérôme* Palaudoux[1*]

[1] Sorbonne Université, CNRS, Laboratoire de Chimie Physique – Matière et Rayonnement, LCP-MR, F-75005 Paris Cedex 05, France
[2] Synchrotron Soleil, 91192 Saint Aubin, France
[3] Université Paris-Saclay, CEA, CNRS, NIMBE, CEA Saclay, 91191 Gif-sur-Yvette, France
[4] Institut de Minéralogie, de Physique des Matériaux et de Cosmochimie, Sorbonne Université, UMR CNRS 7590, MHNH, 75252 Paris, France
[5] Fritz-Haber-Institut der Max-Planck-Gesellschaft, Faradayweg 4-6, 14195 Berlin, Germany
[6] Nano and Molecular Systems Research Unit, University of Oulu, PO Box 3000, FI-90014, Finland
[7] ISMO, CNRS UMR 8214, Université Paris Sud, bâtiment 350, F-91405, Orsay, France

Abstract. We have developed a magnetic bottle time-of-flight electron-electron coincidence spectrometer to perform measurements on solvated molecules in a liquid micro-jet. We present here the first results obtained after ionization of the oxygen 1*s* inner-shell of sodium benzoate molecules and show the possibilities to filter out the electron signal arising from the liquid phase from the signal of water molecules in the gas phase. Both photoelectrons and Auger electrons spectra (unfiltered and filtered) are presented.

1 Introduction

The interaction of high-energy ionizing radiation with matter is still a very interesting and challenging question in many fields. Radiation damage is a complex multi-scale problem, both in spatial and temporal domains. The interactions begin at the atomic level (atto- to femtosecond time scale), then affect the molecular level (femto- to picosecond time scale), and finally can affect cell behavior over hours or days. The early stages of energy deposition processes are crucial for radiobiological damage, as they initiate electron emission processes [1] whereas X-ray photons can cause complex damage to biological samples [2]. In addition to their possible chemical selectivity, they can eject core (photo)electrons from the molecule. This process can be followed by reorganization/relaxation of the electronic structure (possible ejection of additional Auger electrons). All these electrons are new projectiles with given energies, which can interact with the medium and potentially cause new damages [3]. The investigation of such processes in liquid phase is important because biological systems are surrounded by water molecules, most of the time. Experiments in liquid phase are not readily compatible with vacuum due to the high vapor pressure of water which complicates the application of electron spectroscopy. In addition, the low penetration of soft X-ray photons (few micrometers) and the very short propagation lengths of sub keV electrons in

condensed matter (few nanometers) make such studies even more challenging. If in the '70s, electron spectroscopy studies were performed on liquids with a low vapor pressure [4], it is only at the end of the 20th century that Faubel *et al.* studied liquid interfaces using a liquid micro-jet [5]. Since then, many developments occured and liquid micro-jet electron spectroscopy experiments are now common tools [6–9]. Photoelectron spectroscopy provides information about the energies of the emitted electrons, or on the energy dissipation in the solvent (via Coulombic de-excitation or electron transfer phenomena), while photoelectrons / Auger electrons coincidences will provide information on the different relaxation pathways of biomolecules in an aqueous medium and the sharing of energy between the photoelectron and the Auger electrons. This last information may be crucial for increasing the accuracy of the different simulation codes treating the tracks in liquid water like Geant4 [10]. There are several experimental setups where a magnetic bottle – time of flight (MB-TOF) was coupled with a liquid jet (for instance [11,12]), mainly using low repetition rate lasers as ionization sources which could not allow coincidence techniques. Recently, Hergenhahn and co-workers were the first to study electron transfer mediated decay in a lithium chloride solution via electrons coincidences with a MB-TOF using the temporal structure of synchrotron emission [13]. In this work, coincidence measurements were performed by coupling a MB-TOF electron

---

spectrometer with a liquid micro-jet under vacuum together with soft X-ray synchrotron radiation. Filtering of the data will allow identification of the different Auger structures and a better understanding of the effects of the solvent during de-excitation after inner-shell ionization. The first results obtained above the oxygen K-edge will be presented, allowing the liquid phase signal to be separated from the signal of the surrounding gaseous phase via energy filtering of the photoelectrons. Sodium benzoate molecules were used as target since they have already been studied [14], they are harmless and can be used at relative high concentration (1M and more) which is necessary to get a sufficient photoelectron signal.

2 Experimental description

In this project, we used the experimental setup developed by the LCP-MR, which is an evolution of the earlier MB-TOF experimental setup HERMES (High Energy Resolution Multi Electron Spectrometer) developed to study multiple photoionization processes in the gas phase [15–17]. The spectrometer chamber accomodates a titanium tube (90 mm diameter, 1.2 m-length) on which a solenoid is wound (kapton® insulated copper wire) that generates a homogeneous magnetic field (~0.1 mT). The titanium tube is electrically insulated and can be polarized to ac/decelerate the electrons by applying a suitable electric potential. This parameter may be necessary to improve the energy resolution of the spectrometer. A double-layer mu-metal shielding is placed around the drift tube and the interaction chamber. It avoids Earth and external magnetic perturbations that could deviate the electron trajectories. Finally, two turbo-molecular pumps (600 L/s) are added. One is installed at the entrance of the spectrometer, and the other at the end, near the electron detector. This detector uses micro-channel plates (MCP) coupled with delay lines systems for position encoding (Roentdek®). The overall detection efficiency for one electron is estimated to be ~70% [18] which is directly related to the efficiency of the MCP (active surface). The coupling of the MB-TOF with the liquid jet requires many adjustments because of the permanent evaporation of the sample. Namely, the det ector system must be kept under a high vacuum (< 10^{-5} mbar), while the pressure in the micro-jet chamber can reach 10^{-3}-10^{-4} mbar. This vapor phase can be disruptive for coincidence measurements as it significantly increases the density of events generated in the ionization zone. Moreover, given the low penetration of soft X-rays, only the illuminated part of the liquid micro-jet is probed. The magnet's design was adapted to come as close as possible to the micro-jet without losing magnetic strength in the current setup. For this purpose, a soft iron cone (5 mm base-diameter and 20 mm long) is fixed (by the magnetic force) on top of the permanent magnet (NdFeB truncated cone of 24 mm base-diameter) to concentrate the magnetic field lines. It results in a field of ~0.8 T at the tip of the soft iron cone. This magnet assembly is installed on a XYZ motion controlled by three nano-motors for precise

alignment under vacuum. The magnet assembly can be completely removed from the liquid jet holder for the maintenance outside vacuum. Fig. 1 presents a sketch of the setup used in our experiment which is identical to the one described in reference [19]. On the right side of Fig. 1, one can recognize the liquid jet assembly (nozzle and catcher). The conical magnet is placed at a distance of about 1 mm from the liquid jet.
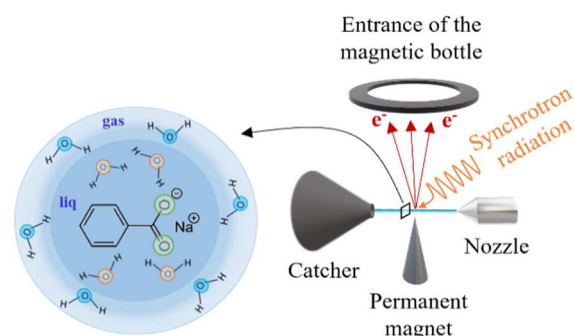

Fig. 1. Scheme of the liquid micro-jet devise coupled with the magnetic bottle electron spectrometer together with a cut view of the liquid and a schematic representation of all types of oxygen atoms present during the measurement.

This assembly is placed in a box that is inserted into the experimental chamber (to maintain the vacuum at a pressure allowing the MCPs to work). The entrance of the magnetic bottle electron spectrometer is located 4 cm above the micro-jet axis and was specially designed with a small 5 mm diameter entrance that allows differential pumping. A manual valve was added to isolate the spectrometer from the experimental chamber in order to decrease the overall venting time when needed.

3 Results at O 1*s* threshold in water (gas and liquid) and discussion

The first measurements were made above the O 1*s* threshold (h*v* = 580 eV). The electrons are decelerated by 20 V. This allows us to separate the photoelectrons from the huge low-energy electrons signal between 0 and 20 eV (not shown here), to recover resolution and reduce the size of the data files (with such deceleration we are not measuring electrons below 20 eV). h*v* + M + retardation (-20 V) → M^{+*} (O 1s^{-1} gas) + e$^-_{ph}$ (~20 eV). The electrons energies are then reset to their correct values (to ease comparison with literature). The M^{+*} excited states will then decay by Auger relaxation (in the case we consider). Thanks to the magnetic bottle time-of-flight electron spectrometer, we can collect all the electrons emitted during an ionization event and detect in coincidence photoelectron and Auger electron. The two-dimensional coincidence map, presenting the coincidences between photoelectrons (y-axis) and Auger electrons (x-axis) is shown in Fig 2. The number of counts (z-axis) is given in the right part of the figure. We observe here more intense zones corresponding to the true coincidences between two electrons. The total electron spectrum is given on the left side of Fig. 2. The

main peak, at 40 eV kinetic energy (blue zone) corresponds to the gaseous water O 1*s* photoelectron whereas the peak at 42 eV kinetic energy (orange zone) corresponds to the liquid water O 1*s* photoelectron. The 2 eV shift between these two photoelectrons' energies is similar to that found in the work of B. Winter [20]. Finally, the faint band at 44 eV (in green) corresponds to the O 1*s* photoelectrons of the benzoate molecule's carboxyl group. The attribution of this peak is consistent with the 1.6 eV shift between the liquid water O 1*s* and the benzoate O 1*s* found in the literature [8]. The low intensity of this band is easy to understand: one molar concentration means that one sodium benzoate molecule is surrounded by 55 water molecules. Sodium benzoate is an amphiphilic molecule, so we do expect that there should be a higher benzoate-to-water ratio at the surface. However, previous studies on sodium benzoate using conventional XPS [14,21] observed that the signal of sodium benzoate remains significantly weaker than that of benzoic acid, its protonated counterpart. It was thus concluded that the surface propensity of sodium benzoate is not so high, thus we may expect an increase of a factor of a few compared to the bulk ratio but not more than an order of magnitude. A precise quantification has not been performed. The observed ratio between the liquid and the gaseous peaks can be explained since the electrons with kinetic energies of a few tens of eV can escape from only a few nm. Other considerations, for instance light polarization should be taken in account.
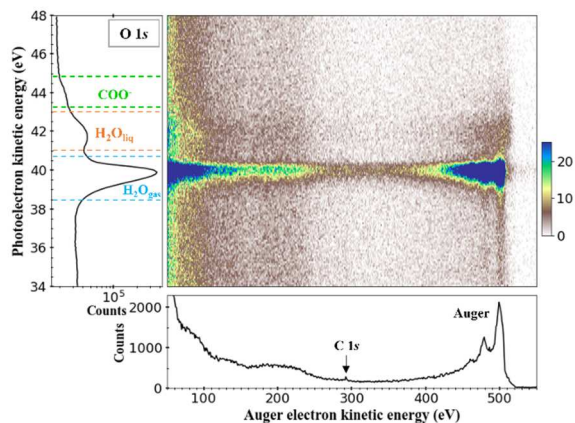
Fig. 2. Sodium benzoate two-dimensional coincidence map « Auger electron kinetic energy / photoelectron kinetic energy » (middle part). The photoelectron spectrum is shown on the left, with a step of 0.1 eV. The total (unfiltered) Auger electron spectrum (lower part, in black) is shown with a step of 1 eV.

The total spectrum (in kinetic energy) obtained by projecting the 2D map data onto the x-axis is given in the lower part of Fig. 2. In this spectrum we can recognize the Auger bands of O 1*s* between 450 eV and 510 eV. These bands are well known but their shape is different from similar spectra in the literature. This point will be discussed later in the manuscript. In this spectrum, one can also point out a peak around 280 eV which is the C 1*s* photoelectron signature. Associated with this peak we distinguish a broad structure between 150 eV and 270 eV which can be associated

(energetically) with the C 1*s* Auger electrons. Such structures can also be associated with secondary electrons generated after oxygen atoms inner-shell ionization, from collisions and from other decay processes (as cascades). Nevertheless, this total electron energy spectrum does not allow to distinguish the Auger relaxations consecutive to the emission of one O 1*s* photoelectron (from gaseous or liquid water or a molecule). Our coincidence measurements allow to select an energy range within the data corresponding to the photoelectron of interest. Projecting this filtered data along the x-axis gives the filtered Auger spectra in Fig. 3.
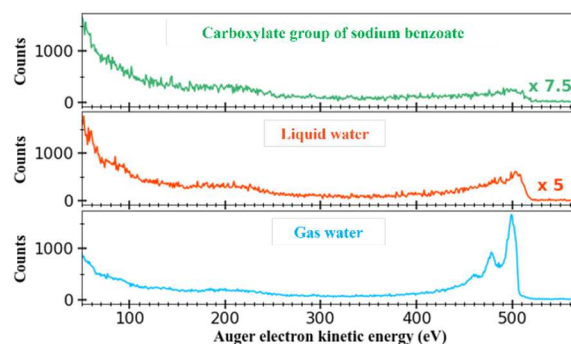
Fig. 3. Photoelectron-filtered spectra with a step of 1 eV, showcasing Auger features. The colors of the spectra refer to the nomenclature of the different oxygens species given in Fig 2. Scaling factors were applied to the liquid and molecular spectra for comparison.

Fig. 3 shows the filtered Auger spectra (in kinetic energy) after ionization of the O 1*s* atom in gaseous water (bottom part of Fig. 3, in blue), liquid water (middle part of Fig. 3, in orange), and in the benzoate molecules (upper part, in green). The colors of the spectra correspond to those chosen for the photoelectrons in Fig. 2. In the gaseous water spectrum (in blue), between 450 eV and 510 eV, one can clearly distinguish the well-known Auger bands of O 1*s* comparable to those in the literature ([22,23] for example). The Auger spectrum from water in the liquid phase (orange) is less clear. Nevertheless, similarities are found such as diminution of the peaks resolution and a 10 eV shift with the main O 1*s* gaseous Auger band as seen by Öhrwall in water clusters [24] suggesting that such media begin to behave like a liquid. Our spectrum remains identical to [8,20] which were obtained after subtraction of the gas phase contribution. However, our coincidence method allows a direct and selective measurement, preventing having data analysis artifact when removing the gas-phase contribution. In the case of benzoate, there is no comparison available in the literature (gas phase, liquid or solid). In the benzoate spectrum, a smaller band is visible in the same energy range as the O 1*s* Auger of liquid water suggesting a similar behavior. On the other hand, a factor of 3 can be seen between the spectrum of gaseous water and the spectra of liquid water and molecule. Similar studies can also be performed at other edges (inner-shells) like C 1*s* for instance. The main purpose for it is also that only the solvent (water in our case) can evaporate from the liquid

jet. The observation of the C 1*s* electron signal is another clear sign of the liquid medium, as described in [19].

4 Conclusion and perspectives

We report here the first results from a new magnetic bottle time of flight spectrometer dedicated to electron spectroscopy of solvated molecules in the liquid micro-jet environment using the electron-electron coincidence technique. In the O 1*s* inner-shell ionization case we have shown that it is possible to distinguish events from the gaseous water phase and the liquid phase (water or benzoate molecules) in the photoelectron spectrum. Strong theoretical support is needed to disentangle the different Auger spectra. After an inner-shell initial vacancy, different de-excitation pathways can occur such as Inter Coulombic Decay, Electron Transfer Mediated Decay, and classical Auger decays (normal + resonant). Cascade processes can also occur within the « normal » Auger decay, where several secondary electrons are emitted (once a more ionized final state threshold, M^{3+}, M^{4+}, … is energetically open). The interactions between the molecules of interest and the molecules of the solvent must be studied in detail. Several molecules of biological interest at different shells (O 1*s*, C 1*s*, N 1*s*, …) could be considered with our coincidence method to obtain cross sections that will be useful as benchmarks for future theoretical studies.

Acknowledgments

Author contributions

C.N. and J.P. designed the research. All authors performed research. L.H., M.F., P.L. I.I. and J.P. analysed the data. M.F., L.H., F.P., I.I., C.N., R.D. and J.P. wrote the paper.

References

1. A. Tilikidis and A. Brahme, Acta Oncologica **33**, 457 (1994).
2. R. Cox, J. Thacker, D. T. Goodhead, W. K. Masson, and R. E. Wilkinson, International Journal of Radiation Biology and Related Studies in Physics, Chemistry and Medicine **31**, 561 (1977).
3. E. Alizadeh, T. M. Orlando, and L. Sanche, Annu. Rev. Phys. Chem. **66**, 379 (2015).
4. H. Siegbahn and K. Siegbahn, Journal of Electron Spectroscopy and Related Phenomena **2**, 319 (1973).
5. B. Winter and M. Faubel, Chem. Rev. **106**, 1176 (2006).
6. R. Dupuy, C. Richter, B. Winter, G. Meijer, R. Schlögl, and H. Bluhm, J. Chem. Phys. **154**, 060901 (2021).
7. M. Ammann, L. Artiglia, and T. Bartels-Rausch, in *Physical Chemistry of Gas-Liquid Interfaces* (Elsevier, 2018), pp. 135–166.
8. M. A. Brown, M. Faubel, and B. Winter, Annu. Rep. Prog. Chem., Sect. C: Phys. Chem. **105**, 174 (2009).
9. R. Signorell and B. Winter, Phys. Chem. Chem. Phys. **24**, 13438 (2022).
10. S. Agostinelli *et al.*, Nuclear Instruments and Methods in Physics Research Section A: Accelerators, Spectrometers, Detectors and Associated Equipment **506**, 250 (2003).
11. N. Kurahashi, S. Thürmer, S. Y. Liu, Y. Yamamoto, S. Karashima, A. Bhattacharya, Y. Ogi, T. Horio, and T. Suzuki, Structural Dynamics **8**, 034303 (2021).
12. I. Jordan, A. Jain, T. Gaumnitz, J. Ma, and H. J. Wörner, Review of Scientific Instruments **89**, 053103 (2018).
13. M. N. Pohl, C. Richter, E. Lugovoy, R. Seidel, P. Slavíček, E. F. Aziz, B. Abel, B. Winter, and U. Hergenhahn, The Journal of Physical Chemistry B **121**, 7709 (2017).
14. N. Ottosson, A. O. Romanova, J. Söderström, O. Björneholm, G. Öhrwall, and M. V. Fedorov, J. Phys. Chem. B **116**, 13017 (2012).
15. H. Iwayama, N. Sisourat, P. Lablanquie, F. Penent, J. Palaudoux, L. Andric, J. H. D. Eland, K. Bučar, M. Žitnik, Y. Velkov, Y. Hikosaka, M. Nakano, and E. Shigemasa, The Journal of Chemical Physics **138**, 024306 (2013).
16. F. Penent, J. Palaudoux, P. Lablanquie, L. Andric, R. Feifel, and J. H. D. Eland, Physical Review Letters **95**, (2005).
17. J. Palaudoux *et al.*, Physical Review A **82**, (2010).
18. K. Fehre *et al.*, Review of Scientific Instruments **89**, 045112 (2018).
19. L. Huart *et al.*, Physical Chemistry Chemical Physics (2022).
20. B. Winter, E. F. Aziz, U. Hergenhahn, M. Faubel, and I. V. Hertel, The Journal of Chemical Physics **126**, 124504 (2007).
21. L. Huart, Inner Shell Ionization Effects on Molecules of Biological Interest in an Aqueous Medium, Sorbonne University, 2022.
22. W. E. Moddeman, T. A. Carlson, M. O. Krause, B. P. Pullen, W. E. Bull, and G. K. Schweitzer, The Journal of Chemical Physics **55**, 2317 (1971).
23. L. Inhester, C. F. Burmeister, G. Groenhof, and H. Grubmüller, The Journal of Chemical Physics **136**, 144304 (2012).
24. G. Öhrwall *et al.*, The Journal of Chemical Physics **123**, 054310 (2005).